Characterization of Conductor-Backed Absorbing Materials Using a Bottom-Filled Rectangular Waveguide

Edward J. Rothwell and Saranraj Karuppuswami

Abstract – A technique is introduced to extract the permittivity and permeability of absorbing materials that are permanently adhered to a conductor backing. A sample is placed into the bottom of a rectangular waveguide, and the transmission and reflection coefficients are measured. Through comparison to a theoretical model for the bottom-filled waveguide, values of μ and ε can be extracted from the measurements. Experimental results match well with values obtained using the standard transmission/reflection method of Nicolson, Ross, and Weir.

1. Introduction

Magnetic radar-absorbing material (MagRAM) is often applied to air vehicles to reduce radar cross section. The performance of the materials must be verified after they are adhered to the conducting aircraft surface; this is generally done in the field. During development, adhered samples are typically excised and measured in the laboratory. In either case, the conductor backing cannot be removed without affecting the properties of the sample under test.

Many techniques have been devised to measure the properties of MagRAM in the laboratory. If there is no conductor backing, the gold standard is the transmission/reflection method of Nicolson, Ross, and Weir (NRW method [1, 2]), which may be implemented using waveguides. Sensitivity to uncertainties in S-parameters and dimensions is, in general, smaller than with other waveguide methods [3]. When a conductor backing is present, waveguide or transmission-line probes may be used [4, 5], but these are often subject to large errors due to measurement uncertainty [4].

The standard NRW test is not possible with a conductor-backed sample, because it assumes a completely filled cross section and transmission is not possible if the sample is conductor backed. This article proposes a new method in which the sample is oriented with the conductor side on the bottom of a rectangular waveguide (Figure 1). Both transmission and reflection can now be measured. The drawback is that the theoretical transmission and reflection coefficients are significantly harder to obtain. A mode-matching solution to the theoretical problem is described, and experimental results reveal that the new approach produces very good results for typical MagRAM.

Manuscript received 3 December 2019.

Edward J. Rothwell and Saranraj Karuppuswami are with Michigan State University, 428 South Shaw Lane, East Lansing, Michigan 48824, USA; e-mail: karuppus@msu.edu.

2. Characterization Method

The conductor-backed sample under test is machined to fit snugly into a rectangular waveguide as shown in Figure 1. A slot is machined into the bottom of the guide with a depth equal to the thickness of the conductor backing, so that the bottom of the sample is aligned with the bottom of the adjacent empty waveguide sections. A filler material is placed above the sample to press-fit the sample to the bottom of the guide; if unneeded, this filler may be assumed to be free space. The reflection coefficient (S_{11}) and transmission coefficient (S_{21}), referred to the $z = 0$ and $z = \Delta$ planes, may be computed theoretically for given values of μ and ε using a mode-matching approach as described later.

Measurements of N_s individual samples are made using a vector network analyzer, with the ith sample measured M_i times. Typically, different samples have different lengths Δ, but the same thickness d. A sensitivity analysis gives some guidance as to the appropriate range of lengths. The Levenberg–Marquardt algorithm is then used to solve the overdetermined system of nonlinear equations given by the differences between the measured and theoretical S-parameters for the unknowns μ and ε.

3. Calculation of the Theoretical S-Parameters

3.1 Mode-Matching Solution

Mode matching is implemented by first expanding the fields in each of the regions $z < 0$, $0 \le z \le \Delta$, and $z > \Delta$ as a series of transverse electric (TE) and transverse magnetic (TM) modal fields. The field incident on the sample is assumed to be the dominant TM_y mode. The reflection coefficient S_{11} is the ratio of the reflected to the incident dominant-mode amplitudes, and the transmission coefficient is the ratio of the amplitude of the dominant mode transmitted into the region $z > \Delta$ to the amplitude of the incident dominant mode. The modal amplitudes are found by applying boundary conditions on the tangential fields at $z = 0$ and $z = \Delta$ and then weighting by field functions to form a system of linear equations. Details of the solution are not included here, but similar problems are described in a variety of sources, including [6]. Importantly, all the terms in the linear equations are given by simple algebraic expressions.

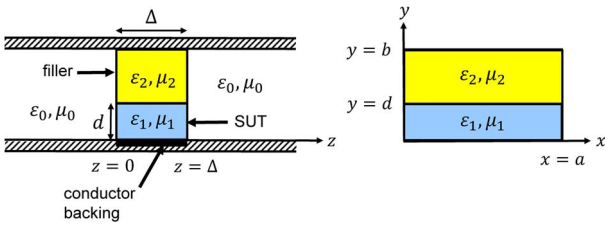

Figure 1. Conductor-backed sample under test placed into a rectangular waveguide. (left) side view; (right) end view.

3.2 Modal Analysis of the Sample Region

The fields in the sample region are found by analyzing an infinitely long rectangular waveguide filled with two materials. Although this is a standard canonical problem covered in many textbooks, computation of the roots of the characteristic equations that define the propagation constants is nontrivial when the materials have arbitrarily complex constitutive parameters. As in [7], the fields may be decomposed into cases that are TE and TM to the y-direction. Noting that the dominant-mode incident field will only couple into modes with similar x-dependence, the characteristic equations may be written in the form

$$\varepsilon_2 \left(k_{y1}^{\mathrm{M}}\right)^2 T_1^{\mathrm{M}} + \varepsilon_1 \left(k_{y2}^{\mathrm{M}}\right)^2 T_2^{\mathrm{M}} = 0 \tag{1}$$

$$\mu_1 T_1^{\mathrm{E}} + \mu_2 T_2^{\mathrm{E}} = 0 \tag{2}$$

for TM and TE modes, respectively. Here,

$$T_1^{\mathrm{M,E}} = \frac{\tan k_{y1}^{\mathrm{M,E}} d}{k_{y1}^{\mathrm{M,E}}}, \quad T_2^{\mathrm{M,E}} = \frac{\tan k_{y2}^{\mathrm{M,E}} (b-d)}{k_{y2}^{\mathrm{M,E}}} \tag{3}$$

and the associated separation equations are

$$\left(\frac{\pi}{a}\right)^2 + \left(k_{y1}^{\mathrm{M,E}}\right)^2 + \left(k_z^{\mathrm{M,E}}\right)^2 = k_1^2 \tag{4}$$

$$\left(\frac{\pi}{a}\right)^2 + \left(k_{y2}^{\mathrm{M,E}}\right)^2 + \left(k_z^{\mathrm{M,E}}\right)^2 = k_2^2 \tag{5}$$

To determine k_{y1} or k_{y2} from a given k_z, a choice must be made on the sign of the square root. This must be done, for instance, during a root search for k_z.

Although the characteristic equations can be written a number of different ways, (1) and (2) are the most expeditious for two reasons. First, it is important that each term be independent of the signs of k_{y1} and k_{y2} arising from the square root; otherwise the root-search algorithm may fail when abrupt sign changes are encountered. Second, writing the trigonometric dependence as tangent functions allows use of the identity

$$\tan z = \frac{1}{j}\frac{e^{jz} - e^{-jz}}{e^{jz} + e^{-jz}} = \frac{1}{j}\frac{1 - e^{-2jz}}{1 + e^{-2jz}} \tag{6}$$

which will not overflow when $\Im\{z\}$ is negative and large. To implement this, the signs of the square roots are chosen such that $\Im\{k_{y1}\} < 0$ and $\Im\{k_{y2}\} < 0$. This is important because the material under test may have a large electric or magnetic loss tangent.

3.3 Numerical Solution to the Characteristic Equations

A propagation constant $k_z^{\mathrm{M,E}}$ is associated with propagating modes when its real part is significantly larger than its imaginary part, and with evanescent modes when the opposite is true. For typical MagRAM, all modes are clearly either propagating or evanescent. Modes are numbered sequentially according to the increasingly negative value of their imaginary part. In implementing the mode-matching technique, a certain number of modes N is chosen with which to expand the fields. It is crucial that all modes numbered less than or equal to N be included. If just a single mode is missed, the accuracy of the solution is highly degraded. Thus, care must be taken to find all the required modes.

The distribution of the propagation constants in the complex plane makes it difficult to use standard techniques, such as Newton's method, to solve the characteristic equations. These methods require very accurate initial guesses, which are difficult to come by without knowing the constitutive parameters of the sample. As an example, consider Figure 2, which shows the first 24 modes for a typical MagRAM (Eccosorb FGM-125) with representative constitutive parameters and an air filler above. Clearly there are two propagating modes, and the remaining modes are evanescent. However, the positions of the roots in the complex plane are difficult to predict.

To be certain of obtaining all the desired roots, a global search algorithm is used, based on computing the number of zeros of an analytic function [8]. If C is a simple closed contour (taken in the positive sense) and $f(z)$ is a function that is analytic on C and analytic within C except at a finite number of poles, then [9]

$$\frac{1}{2\pi j}\int_C \frac{f'(z)}{f(z)}\,dz = M - P \tag{7}$$

Here M is the number of zeros of the function within C, and P is the number of poles within C. Since there are no poles of the characteristic equations in the regions where the zeros are found, (7) may be used to find the number of zeros in a selected region of the complex plane.

The procedure for finding the desired roots is to repeatedly section the complex plane into rectangular boxes and use (7) to find the number of roots in each box. Those boxes with roots are sectioned until the boxes are small enough to guarantee convergence of Newton's method using the center of the box as an initial guess. Conveniently, the ratio $f'(z)/f(z)$ also appears in Newton's method, and the derivative $f'(z)$ can be computed in closed form. In addition, the integrals around the periphery of the rectangular boxes can be computed as integrals of a single real variable through appropriate parameterization and with knowl-

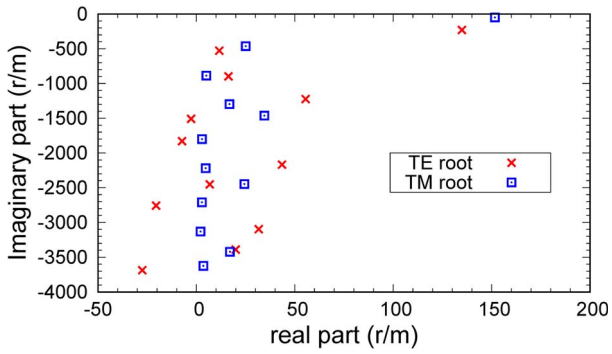

Figure 2. First 24 roots of the characteristic equations. $f = 10$ GHz, $d = 3.175$ mm (0.125 inch), $\varepsilon_r = 7.32 - j0.0464$, $\mu_r = 0.576 - j0.484$.

edge that the result is real. A relatively crude approximation to the integrals may be used since it is known a priori that (7) yields a nonnegative integer. Note that all terms in the derivative are independent of the sign chosen on the square root to determine k_y.

3.4 Convergence of the Mode-Matching Solution

The accuracy of the mode-matching solution depends on the number of modes used to represent the fields. As the number of modes N is increased, the values of the S-parameters appear to oscillate and slowly converge as N gets large. However, if the trend is examined as N is increased by 4, then a smooth convergence appears, as seen for the phase of S_{21} in Figure 3. In fact, polynomial extrapolation can be used to accurately predict the S-parameters for $N \to \infty$. A fourth-order polynomial passed through $N = 23$, 27, 31, 35 gives excellent results for typical MagRAM, as shown in Figure 3. The final results match those from the commercial solver HFSS to five digits in magnitude and phase across the X band.

4. Experimental Results

As a proof of concept, a commercial MagRAM sample (Eccosorb FGM-125) was measured in the laboratory. This material shows significant absorption in

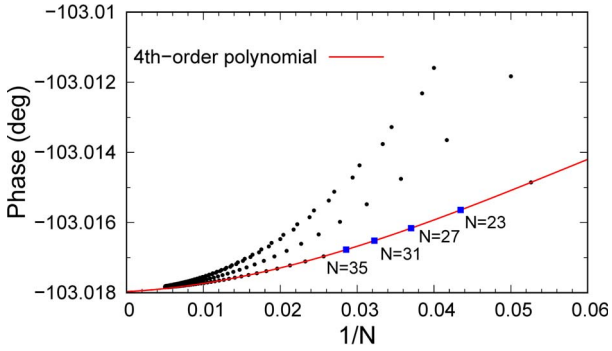

Figure 3. Convergence of the phase of S_{21}. $f = 10$ GHz, $d = 2.54$ mm (0.1 inch), $\Delta = 10.16$ mm (0.4 inch), $\varepsilon_r = 7 - j0.1$, $\mu_r = 0.5 - j0.5$.

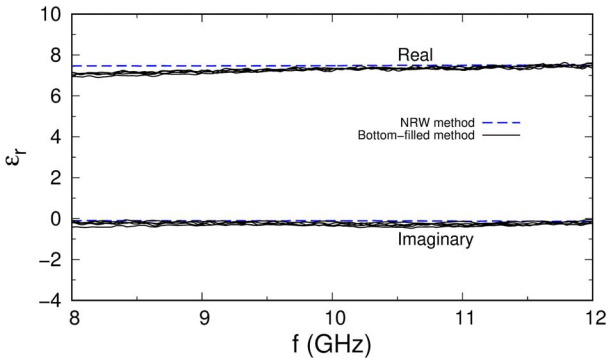

Figure 4. Relative permittivity extracted from five measured data sets. Results are shown for each data set.

the band 2–12 GHz, and we and others have used it to test material characterization systems and algorithms [10–12].

The sample was cut, sanded smooth, and placed into the bottom of an X-band waveguide. The dimensions of the finished sample were measured using a micrometer and found to be $\Delta = 5.1308$ mm, $d = 2.6670$ mm. Note that for this test there was no conductor backing, but the position of the sample mimics the effect of the conductor backing of an actual sample being placed into a slot in the bottom of the guide. A piece of polystyrene foam was inserted above the sample to press-fit the sample against the bottom wall.

Values of μ and ε for both the MagRAM and foam were first measured using the NRW approach with cross-section-filling samples. The foam was found to have a value of $\mu_r = 1$ and $\varepsilon_r = 1.028 - j0.0006$, with little variation across the band. Next, the cut sample was placed on the bottom of the waveguide and measured five times, with the system calibrated before each measurement. Finally, values of μ and ε were extracted for the cut sample using the Levenberg–Marquardt algorithm. As a part of the NRW method, the one-way absorption of the dominant waveguide mode by the cross-section-filling sample, $20\log_{10}|e^{-jk_z d}|$, is easily computed. It was found to vary from −5.8 dB at 8 GHz to −3.2 dB at 12 GHz. This shows that the material demonstrates significant absorption across the X band.

Figures 4 and 5 compare the NRW results to the bottom-filled results for μ and ε, extracted one data set at a time. The average of the five individual extracted values is, to within three digits, the same as the value extracted with the Levenberg–Marquardt algorithm using all five data sets at once. The standard deviation in ε_r averaged across the band is 0.05 for the real part and 0.07 for the imaginary part. The maximum absolute difference between ε_r for the NRW and bottom-filled methods is 0.42 in the real part and 0.22 in the imaginary part. This corresponds to a maximum 6.2% difference in magnitude. The percent difference in angle is much larger, since the imaginary part of ε_r is very small and thus difficult to determine with high accuracy. The standard deviation in μ_r averaged across the band is

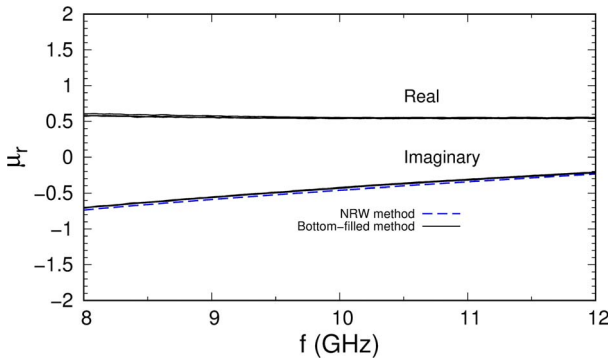

Figure 5. Relative permeability extracted from five measured data sets. Results are shown for each data set.

0.008 for the real part and 0.004 for the imaginary part. The maximum absolute difference between μ_r for the NRW and bottom-filled methods is 0.028 in the real part and 0.035 in the imaginary part. This corresponds to a maximum 2.0% difference in magnitude and 9.4% difference in angle. At midband (10 GHz), the extracted relative permeability using the NRW method with all five data sets is $0.533 - j0.460$, which compares to $0.546 - j0.425$ using the proposed method, while the extracted relative permittivity of $7.48 - j0.105$ from the NRW method compares to $7.31 - j0.293$ for the proposed method.

5. Comments and Conclusions

The measured results shown in Figures 4 and 5 are, in our experience, considerably better than those produced by other waveguide techniques. The source of the error is probably variation in the dimensions of the sample and imperfect knowledge of the permittivity of the foam filler. The sample was sanded as carefully as possible, but some surface variability remained. Sensitivity analysis revealed that an uncertainty of 0.0254 mm (1 mil) in the sample thickness can produce as much as a 10% error in the real part of ε, depending on the values of Δ and d. Similarly, an uncertainty in the relative permittivity of the foam filler of 0.001 can produce a 5% error in the real part of ε. In fact, if the foam is assumed to have the properties of free space, the extracted real part of ε has a value of approximately 5 across the band (a difference from the NRW results of over 30%). Fortunately, both the real and imaginary parts of μ are far less sensitive to uncertainties in these parameters. Thus, although the present method is capable of producing accurate results for ε, care must be taken to control the uncertainties in dimensions and filler permittivity.

6. Acknowledgment

The authors are grateful to Benjamin Crowgey for numerous discussions regarding the measurement of conductor-backed materials, and for providing feedback on the manuscript.

7. References

1. A. M. Nicolson and G. F. Ross, "Measurement of the Intrinsic Properties of Materials by Time-Domain Techniques," *IEEE Transactions on Instrumentation and Measurement*, **19**, 4, November 1970, pp. 377–382.
2. W. B. Weir, "Automatic Measurement of Complex Dielectric Constant and Permeability at Microwave Frequencies," *Proceedings of the IEEE*, **62**, 1, January 1974, pp. 33–36.
3. R. A. Fenner, E. J. Rothwell, and L. L. Frasch, "A Comprehensive Analysis of Free-Space and Guided-Wave Techniques for Extracting the Permeability and Permittivity of Materials Using Reflection-Only Measurements," *Radio Science*, **47**, 1, February 2012, pp. 1–13.
4. G. D. Dester, E. J. Rothwell, M. J. Havrilla, and M. Hyde IV, "Error Analysis of a Two-Layer Method for the Electromagnetic Characterization of Conductor-Backed Absorbing Materials Using an Open-Ended Waveguide Probe," *Progress in Electromagnetic Research B*, **26**, 1, 2010, pp. 1–21.
5. M. W. Hyde IV, J. W. Stewart, M. J. Havrilla, W. P. Baker, E. J. Rothwell, and D. P. Nyquist, "Nondestructive Electromagnetic Material Characterization Using a Dual Waveguide Probe: A Full Wave Solution," *Radio Science*, **44**, 3, June 2009, pp. 3013–3026.
6. E. J. Rothwell and M. J. Cloud, *Electromagnetics*, 3rd ed., Boca Raton, FL, CRC Press, 2018.
7. R. F. Harrington, *Time Harmonic Electromagnetic Fields*, New York, McGraw-Hill, 1961.
8. M. Dellnitz, O. Schütze, and Q. Zheng, "Locating All the Zeros of an Analytic Function in One Complex Variable," *Journal of Computational and Applied Mathematics*, **138**, 2, January 2002, pp. 325–333.
9. R. V. Churchill, J. W. Brown, and R. F. Verhey, *Complex Variables and Applications*, 3rd ed., New York, McGraw-Hill, 1974.
10. M. W. Hyde, M. J. Havrilla, and A. E. Bogle, "A Novel and Simple Technique for Measuring Low-Loss Materials Using the Two Flanged Waveguides Measurement Geometry," *Measurement Science and Technology*, **22**, 8, July 2011, p. 085704.
11. G. D. Dester, E. J. Rothwell, and M. J. Havrilla, "Two-Iris Method for the Electromagnetic Characterization of Conductor-Backed Absorbing Materials Using an Open-Ended Waveguide Probe," *IEEE Transactions on Instrumentation and Measurement*, **61**, 4, April 2012, pp. 1037–1044.
12. M. W. Hyde and M. J. Havrilla, "Simple, Broadband Material Characterization Using Dual-Ridged Waveguide to Rectangular Waveguide Transitions," *IEEE Transactions on Electromagnetic Compatibility*, **56**, 1, February 2014, pp. 239–242.